

SPEAR: Early results from a very high latitude ionospheric heating facility

T. K. Yeoman^a, N. Blagoveshchenskaya^b, V. Kornienko^b, T. R. Robinson^a, R. S. Dhillon^a, D. M. Wright^a, and L. J. Baddeley^a

^a*Department of Physics and Astronomy, University of Leicester, LE1 7RH, UK.*

^b*Arctic and Antarctic Research Institute (AARI), 199397, St. Petersburg, Russia.*

Abstract

Early results are presented from high power ionospheric modification experiments with the SPEAR (Space Plasma Exploration by Active Radar) HF facility, which is used to generate artificial field-aligned irregularities (AFAI) in the polar cap ionosphere. These AFAIs are detected both through HF coherent backscatter radar and bistatic HF Doppler experiments. The AFAIs created with SPEAR are demonstrated to provide an important geophysical diagnostic of the polar cap ionospheric electric field, and may also scatter radio waves out of the ionospheric waveguide, even when they have propagated over very considerable distances.

1. Introduction

High power radio wave facilities such as the EISCAT Heating facility at Tromsø, Norway (Rietveld et al., 1993) provide a highly flexible tool for investigating fundamental plasma physics and geophysical phenomena. It is well known that O-mode heating is capable of generating artificial field aligned irregularities (AFAI) using high power HF radio waves (e.g. Hedberg et al., 1983; Djuth et al., 1985; Blagoveshchenskaya and Troshichev, 1996; Yampolski et al., 1997; Blagoveshchenskaya et al., 1998; Eglitis et al., 1998; Robinson, 1989; Rietveld et al., 2003). These irregularities are detectable by both incoherent and coherent scatter radars (e.g. Robinson et al., 1997). The striations are thought to be generated by a thermal parametric instability at the upper-hybrid resonance (UHR) height, although they extend for several tens of kilometres along the geomagnetic field (Robinson, 1989). AFAI provide a powerful source of coherent backscatter for HF radars, where the heater-induced scatter is usually very much stronger than scatter of natural origin e.g. Bond et al. (1997). The Doppler shift imposed on the AFAI by oscillations in the background convection electric field in which the AFAI are imbedded provide a valuable diagnostic of geophysical phenomena. Such Doppler-shifted signals may be detected by both HF backscatter systems (e.g. Yeoman et al., 1997) and bistatic HF Doppler experiments (e.g. Blagoveshchenskaya et al., 1998). Previously, such experiments were restricted to the auroral zone and lower latitudes, but the new SPEAR (Space Plasma Exploration by Active Radar) HF facility (Robinson et al., 2006) now allows for such experiments in the polar cap. The results presented here illustrate the capability of the SPEAR high-power beam to generate artificial field-aligned irregularities (AFAI).

2. Experimental arrangement

SPEAR (Space Plasma Exploration by Active Radar) is a new high-power radar system located at 78.15° N latitude, 16.05° E longitude, in the vicinity of Longyearbyen (Spitzbergen) and is designed to carry out a range of space plasma investigations of the polar ionosphere and magnetosphere. The SPEAR site is located adjacent to the EISCAT Svalbard Radar (ESR). The SPEAR antenna system comprises a 6×4 array of full-wave, crossed-dipoles, 16m above the ground, with an antenna spacing of 48.4m, allowing the transmission of both linear and circularly polarised signals. The individual dipoles are rhombically broadened to allow operation between 4 and 6 MHz. The resulting beam has a quasi-elliptical cross-section, with an average half-power width of 21° along its major axis and 14° along its minor axis. This results in an overall antenna gain of 21 dB. Individual phase-control provides beam-steering within ±30° from zenith, at any

azimuth, without significantly altering the antenna gain or introducing significant side-lobe signals. The beam may thus be pointed in directions which include vertical and field-aligned. Beam-steering to angles further from the zenith may be achieved but in this case significant side-lobes are introduced into the radiation pattern. SPEAR has a distributed transmitting and receiving system consisting of individual 4-kW solid-state transmitters connected to the antenna array. Each transmitter consists of a single driver-stage and 4 individual 1-kW modules, the outputs of which are combined and fed to the antenna. In the 4×6 configuration 48 such transmitters are required. These are made up of 192 power-amplifier modules, 48 driver stages and a total of 240 power-supply units. Each transmitter contains an embedded controller and an individual Direct Digital Synthesiser (DDS) which provides a transmit signal and the IF for the receiver front-end. During the operations reported here the complete 6×4 SPEAR array was available (48 transmitters), operating at 4.45 MHz, which produced an antenna gain of 21 dB. The transmitters were operated at 2 kW, resulting in an Effective Radiated Power (ERP) for SPEAR of ~ 15 MW.

The SPEAR site is within the fields of view of both the CUTLASS radars at Hankasalmi, Finland and Þykkvibær, Iceland, which are routinely operated throughout SPEAR experiments and are ideally situated for making observations of AFAI in the SPEAR-modified ionosphere over the ESR. The stereo-CUTLASS radar is an HF coherent backscatter radar system, capable of near simultaneous operation on two separate frequencies (Lester et al., 2004). The radars form part of the SuperDARN array (Greenwald et al., 1995). Both radars reach the ionosphere above SPEAR via a 1.5-hop HF propagation path. Normal operations for both radars involve a 16-beam scan over ranges 180–3555 km, with an integration time of 3 or 6 s providing a full-scan time resolution of 1 or 2 min. In the experiments presented here the CUTLASS radars ran in a high temporal and spatial resolution mode, with both radars running a reduced scan of 3–5 beams centred over SPEAR (beams 6 and 9 for Þykkvibær and Hankasalmi respectively), with an integration time of 1 s. Channel-A of each of the radars provides high spatial resolution, with a field-of-view restricted to 75 range-gates of size 15 km covering ranges of 1485–2610 km, while Channel-B provides data over the complete propagation path from the HF radars to SPEAR at a resolution of 45 km, over distances of 180–3555 km. The viewing geometry of Channels A and B for Hankasalmi and Þykkvibær are illustrated in Fig. 2. Both Channels A and B of each radar additionally perform a small frequency sweep, with the scans cycling through approximately three HF frequencies which are appropriate to allow propagation to Svalbard over a 1.5-hop path. Frequencies of 11–13 MHz were chosen for the experiments presented here. Thus the combination of the integration-time, scan-pattern and frequency-sweep provided a time-resolution of between 9 and 15 s in this arrangement. Simultaneous bistatic HF Doppler measurements are also available from four channels recorded at St. Petersburg (SPB). The HF diagnostic signals from broadcasting stations at Pori (Finland, 11.755 MHz) and London (BBC stations, 17.64 MHz) were recorded, along with the SPEAR frequency and its second harmonic (4.45 and 8.90 MHz) to analyse possible self-scattering effects (Yampolski et al., 2005). The geometry of the bistatic HF Doppler experiments is illustrated in Fig. 2 which shows the "direct" paths London-SPB and Pori-SPB (thin lines) where signals propagate from the transmitter to the receiver along a great circle path. Scattered paths correspond to the London-SPEAR-SPB and Pori-SPEAR-SPB paths (thick lines). The mechanism of bi-static scatter is very similar to the backscatter recorded at CUTLASS, but with the transmitter and receiver at different locations.

3. Results

Data from SPEAR-induced AFAI detected in the CUTLASS Þykkvibær radar on 1 October 2004 between 12:00 and 14:00 UT are presented in Fig. 3. The Doppler velocity of the AFAI is presented as a function of geographic longitude and time for Þykkvibær beam 6. Spear was transmitting a 4 min on, 4 min off O-mode cycle, represented in Fig. 3 by vertical lines, and AFAI can clearly be observed, centred on Þykkvibær range gate 45, $20^\circ - 24^\circ$ geographic longitude, when SPEAR was transmitting. This apparent range is shifted somewhat eastward of the true longitude of

SPEAR, due to group retardation of the HF propagation path from Þykkvibær to SPEAR. The line of sight velocity data shows a consistent drift towards the radar of $0 - 400 \text{ m s}^{-1}$, resulting from the $\mathbf{E} \times \mathbf{B}$ drift imposed by the ionospheric convection electric field. AFAI induced by the SPEAR system may similarly be diagnosed from bi-static HF Doppler scatter observations. Figure 4 presents a dynamic Doppler spectrum of received signal strength from bi-static HF Doppler scatter observations on the London-SPEAR-St.Petersburg path on 31 Jan 2006 between 17:12 and 17:48 UT. The time intervals when SPEAR was transmitting are marked by vertical bars on the time axis. Spear was again transmitting an O-mode signal, but this time a 2 min on, 2 min off cycle was employed. Zero Doppler frequency corresponds to the direct signals propagating from the transmitter to the receiver along a great-circle path. Signals scattered from SPEAR-induced field-aligned small-scale irregularities are recorded as additional tracks shifted in frequency from that of the direct signals at zero Doppler frequency. Positive Doppler frequency shifts correspond to a southward motion of irregularities (toward the reception point) and negative Doppler frequency values correspond to a northward motion (away from the receiver). Well-defined signals scattered from AFAI generated at SPEAR are recorded as additional tracks shifted by $\sim +3 \text{ Hz}$ Doppler frequency (equivalent to a line-of-sight horizontal irregularity velocity in the direction of the bisector of the HF radio propagation paths of $\sim 30 \text{ m s}^{-1}$), visible only when SPEAR is transmitting.

Figure 5 presents dynamic Doppler spectra of the received signals on the SPEAR-St. Petersburg and Botswana (southern Africa)-SPEAR-St. Petersburg paths for data taken on 29 Jan 2006, 18:50 - 19:50 UT. SPEAR was again transmitting at 4.45 MHz, using O-mode polarisation with a 2 min on, 2 min off cycle. In this case data from the SPEAR-St. Petersburg propagation path are presented in the left hand panel. This direct propagation path clearly illustrates the on/off cycles of the SPEAR high power transmissions, and in this case therefore contains no Doppler frequency shifts. A weaker trace is visible from 19:00 - 19:20 UT at a frequency shift of 4 Hz, presumably due to an additional propagation path where a motion of the reflecting ionosphere (perhaps due to a gravity wave, applies a frequency shift. Bistatic HF Doppler scatter observations, this time from a Botswana-SPEAR-St. Petersburg path at 17.895 MHz are presented in the right hand panel. Here zero Doppler frequency corresponds to the direct signals propagating from the diagnostic transmitter at Botswana to the receiver at St. Petersburg along a great circle path. One can see that the direct signals were very weak. At the same time strong scattered signals from the bistatic path are recorded shifted by about -3.5 Hz Doppler frequency (equivalent to a line-of-sight horizontal irregularity velocity in the direction of the bisector of the HF radio propagation paths of $\sim 35 \text{ m s}^{-1}$). These scattered signals were only observed during SPEAR-on times when scattering from SPEAR-induced AFAI occurs.

4. Discussion

Fig.3 presented data from SPEAR-induced AFAI detected in the CUTLASS Þykkvibær radar on 1 October 2004 between 12:00 and 14:00 UT. The AFAI act as very coherent artificial targets for HF radars such as CUTLASS, and have been demonstrated to accurately track the natural ionospheric convection velocity (Eglitis et al., 1998). The backscatter obtained is of very high power and very narrow spectral width. This allows a short integration time to be run on the radar, providing higher time resolution than is normally available. The narrow spectral widths also produce ionospheric electric field measurements of unprecedented accuracy. Combining common-volume data from the CUTLASS Hankasalmi and Þykkvibær radars then allows a vector velocity determination. This has been done with the EISCAT heater at Tromsø, (Yeoman and Wright, 2001) and is now possible for the first time over the EISCAT Svalbard radar.

Figure 4 presented data from 31 Jan 2006 between 17:12 and 17:48 UT. Well-defined signals scattered from AFAI generated at SPEAR are recorded as additional tracks shifted by $\sim +3 \text{ Hz}$ Doppler frequency, visible only when SPEAR is transmitting. Some variability in the Doppler shift of the scattered signals can be seen during the interval presented, presumably resulting from variability in the convection electric field, which imposes a drift velocity on the AFAI, and hence a

Doppler shift on the received signal. In addition to the Doppler variability of the scattered signals, small frequency variations in the directly-propagating signal can also be seen. These are most likely due to frequency shifts imposed on the propagation path by naturally occurring ULF waves of magnetospheric origin. Such oscillations are frequently observed on both near-vertical HF Doppler sounders, and on ground scatter from SuperDARN HF radar data (Menk et al., 2003). The amplitude of frequency variations in both direct great circle signals and signals scattered from AFAI at SPEAR are small, only about 1 Hz, but the frequency resolution is 0.1 Hz, so we can be confident that these Doppler frequency shift variations are real. For the time periods displayed in Figs. 4 and 5, no artificial backscatter data were available from the CUTLASS radars, as no propagation path was viable between the radars and the ionosphere overlying SPEAR. This illustrates the difficulty in performing HF experiments over such large ranges, and also illustrates the value of having more than one HF propagation path for the diagnosis of the ionospheric modification experiments performed at SPEAR. Figure 6 illustrates the median Doppler frequency shifts for signals scattered from SPEAR-induced AFAI on the London-SPEAR-St. Petersburg path obtained from the dynamic Doppler spectra in Fig. 4. The Doppler frequency shift measurements during each 2 min on interval can be seen to be very consistent. However a systematic variation is seen in the Doppler shift over the ~30 min interval covered in Fig. 6, as the convection electric field varies over this longer interval.

Figure 5 presented data from the direct SPEAR-St. Petersburg propagation path and bi-static HF Doppler scatter observations, this time from a Botswana-SPEAR-St. Petersburg path on 29 Jan 2006, 18:50 – 19:50 UT. Here the diagnostic signal received at St. Petersburg was at 17.895 MHz, from a transmitter located in Botswana, some 10 000 km from the SPEAR site. Thus propagation over such a large distance was presumably through an ionospheric wave-guide. The removal from wave-guide then occurred when the signal impinged on the AFAIs produced by SPEAR, and the scattered signals were subsequently detected by the SPB receiver. This illustrates the immense variety of HF propagation paths which can be utilised for the diagnosis of the effects of high power ionospheric modification experiments at SPEAR. High power SPEAR campaigns are now running routinely four times a year, and significant further progress in plasma physics and geophysical experiments is anticipated over the next few years of operations.

Acknowledgments.

SPEAR is supported by PPARC grant PP/E002544/1, RSD and LJB are supported by PPARC grant PPA/G/O/2003/00013.

References

- Blagoveshchenskaya, N.F., and Troshichev, O.A.: Ionospheric phenomena produced by modification experiments, *J. Atmos. Terr. Phys.*, 58, 397-406, 1996.
- Blagoveshchenskaya N. F., V. A. Kornienko, A. V. Petlenko, A. Brekke, and M. T. Rietveld, Geophysical phenomena during an ionospheric modification experiment at Tromsø, *Ann. Geophys.* 16, 1212–1225, 1998.
- Bond, G., T. R. Robinson, P. Eglitis, D. M. Wright, A. J. Stocker, M. T. Rietveld, and T. B. Jones, Spatial observations by the CUTLASS coherent scatter radar of ionospheric modification by high power radio waves, *Ann. Geophys.*, 15, 1412–1421, 1997,
- Djuth, F.T., Jost, R.J., Noble, S.T., Gordon, W.E., Stubbe, P., Kopka, H., Nielsen E., Bostrøm, R., Derblom, H., Hedberg, A., and Thide, B.: Observations of E region irregularities generated at auroral latitudes by a high power radio wave, *J. Geophys. Res.*, 90, 12293–12306, 1985.
- Eglitis, P., T. R. Robinson, M. T. Rietveld, D. M. Wright, and G. E. Bond, The phase speed of artificial irregularities observed by CUTLASS during HF modification of the auroral ionosphere, *J. Geophys. Res.*, 103, 2253, 1998.

- Greenwald, R. A., K. B. Baker, J. R. Dudeney, M. Pinnock, T. B. Jones, E. C. Thomas, J.-P. Villain, J.-C. Cerisier, C. Senior, C. Hanuise, R. D. Hunsucker, G. Sofko, J. Koehler, E. Nielsen, R. Pellinen, A. D. Walker, N. Sato, and H. Yamagishi, DARN/SuperDARN: A global view of the dynamics of high latitude convection, *Space Sci. Rev.*, **71**, 761–796, 1995.
- Hedberg, A., Derblom, H., Thide, B., Kopka, H., and Stubbe, P.: Observations of HF backscatter associated with the heating experiment at Tromsø, *Radio Sci.*, **18**, 840–850, 1983.
- Lester, M., P. J. Chapman, S. W. H. Cowley, S. J. Crooks, J. A. Davies, P. Hamadyk, K. A. McWilliams, S. E. Milan, M. J. Parsons, D. B. Payne, E. C. Thomas, J. D. Thornhill, N. M. Wade, T. K. Yeoman, and R. J. Barnes, Stereo CUTLASS: A new capability for the SuperDARN radars, *Ann. Geophys.*, **22**, 459–473, 2004,
- Menk, F. W., T. K. Yeoman, D. Wright, M. Lester, and F. Honary, High latitude observations of impulse-driven ULF pulsations in the ionosphere and on the ground, *Ann. Geophysicae*, **21**, 559–576, 2003.
- Rietveld, M. T., H. Kohl, , H. Kopka, , and P. Stubbe, , Introduction to ionospheric heating at Tromsø – I. Experimental overview, *J. Atmos. Terr. Phys.*, **55**, 577, 1993.
- Rietveld, M.T., Kosch, M.J., Blagoveshchenskaya, N.F., Kornienko, V.A., Leyser, T.B., and Yeoman, T.K.: Ionospheric electron heating, aurora and striations induced by powerful HF radio waves at high latitudes: aspect angle dependence, *J. Geophys. Res.*, **108**(A4), 1141, doi:10.1029/2002JA009543, 2003.
- Robinson, T. R.: The heating of the high latitude ionosphere by high power radio waves, *Phys. Rep.* **179**, 79–209, 1989.
- Robinson, T. R., A. J. Stocker, G. Bond, P. Eglitis, D. M. Wright, and T. B. Jones, O and X mode heating effects observed simultaneously with the CUTLASS and EISCAT radars and low power HF diagnostics at Tromsø, *Ann. Geophys.*, **15**, 134–136, 1997.
- Robinson T. R., T. K. Yeoman, R. S. Dhillon, M. Lester, E. C. Thomas, J. D. Thornhill, D. M. Wright, A. P. van Eyken and I. W. McCrea, First observations of SPEAR-induced artificial backscatter from CUTLASS and EISCAT Svalbard radars, *Ann. Geophys.*, **24**, 291–309, 2006.
- Yampolski, Y.M., Beley, V.S., Kasheev, S.B., Koloskov, A.V., Somov, V.G., Hysell, D.L., Isham, B., and Kelley, M.C.: Bistatic HF radar diagnostic induced field-aligned irregularities, *J. Geophys. Res.*, **102**(A4), 7461–7467, 1997.
- Yampolski, Yu. M., A.V Zalizovski, V.G. Galushko, A.V. Koloskov, S.B. Kascheev, Self scattering effect of powerful HF radiation as observed in Europe and Antarctica, proceedings of RF Ionospheric Interactions Workshop, Santa Fe, New Mexico, pp. 31 – 38, 2005.
- Yeoman, T. K. and D. M. Wright, ULF waves with drift resonance and drift-bounce resonance energy sources as observed in artificially-induced HF radar backscatter, *Ann. Geophys.* **19**, 159–170, 2001.
- Yeoman, T. K., D. M. Wright, T. R. Robinson, and M. T. Rietveld, High spatial and temporal resolution observations of an impulse-driven field line resonance in backscatter radar artificially generated with the Tromsø heater, *Ann. Geophys.*, **15**, 634–644, 1997.

Figure captions

Figure 1. The viewing geometry of the high spatial resolution and standard channels of the Hankasalmi, (left panel) and Pykkvibær (right panel) CUTLASS HF coherent scatter radars when operated with the SPEAR high power facility on Svalbard.

Figure 2. The geometry of the SPEAR-bistatic HF Doppler experiments

Figure 3. HF radar measurements of the Doppler velocity of AFAI induced by the SPEAR system, presented as a function of geographic longitude and time for Pykkvibær beam 6. Spear was

transmitting a 4 min on, 4 min off O-mode cycle, represented by vertical lines, and AFAI can clearly be observed, centred on Þykkvibær range gate 45, $20^{\circ} - 24^{\circ}$ geographic longitude.

Figure 4. A dynamic Doppler spectrum of received signal strength from bi-static HF Doppler scatter observations on the London-SPEAR-St.Petersburg path on 31 Jan 2006 from 17:12 to 17:48 UT. Spear was transmitting a 2 min on, 2 min off O-mode cycle, represented by vertical bars. Zero Doppler frequency corresponds to the direct signals propagating from the transmitter to the receiver along a great-circle path. Scattered signals are recorded as additional tracks shifted by $\sim +3$ Hz Doppler frequency.

Figure 5. Dynamic Doppler spectra of the received signals on the SPEAR-St. Petersburg (left hand panel) and Botswana (southern Africa)-SPEAR-St.Petersburg (right hand panel) paths for data taken on 29 Jan 2006, 18:50 – 19:50 UT. Spear was transmitting at 4.45 MHz, using O-mode polarisation, with a 2 min on, 2 min off cycle. Zero Doppler frequency in each panel corresponds to the direct signals propagating from the transmitter to the receiver along a great-circle path. Scattered signals from the bistatic path are recorded, shifted by ~ -3.5 Hz Doppler frequency, in the right hand panel.

Figure 6. The measured Doppler frequency shift from the bi-static HF Doppler observations on the London-SPEAR-St.Petersburg path, as presented in the dynamic spectrum in Figure 4.

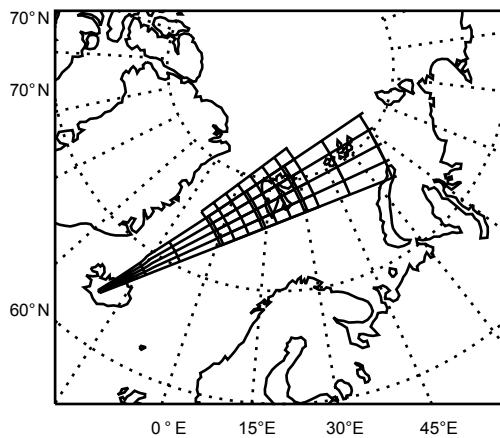
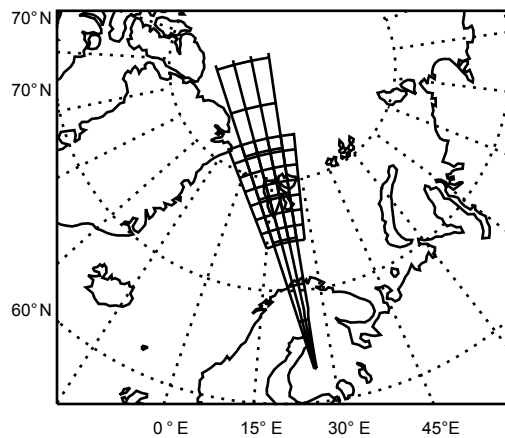


Figure 1

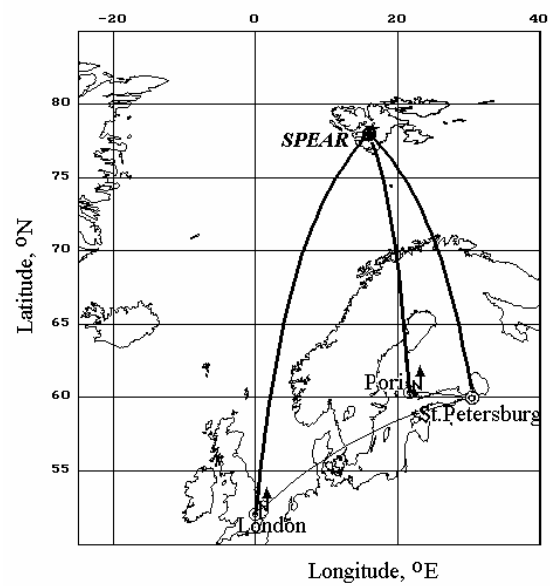


Figure 2

SPEAR and CUTLASS

Pykkvibaer Rg 45

1 Oct 2004 ⁽²⁷⁵⁾

unknown scan mode (-26401)

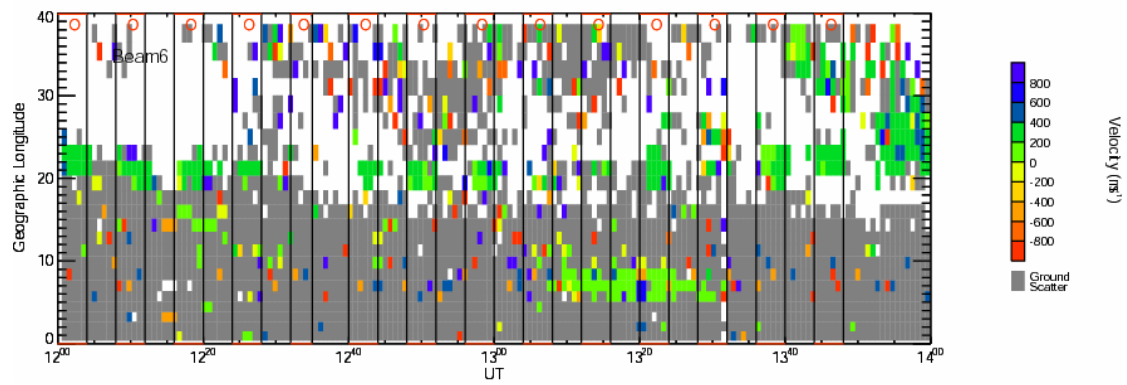


Figure 3

January 31, 2006, $f = 17640$ kHz

London - SPEAR - St. Petersburg

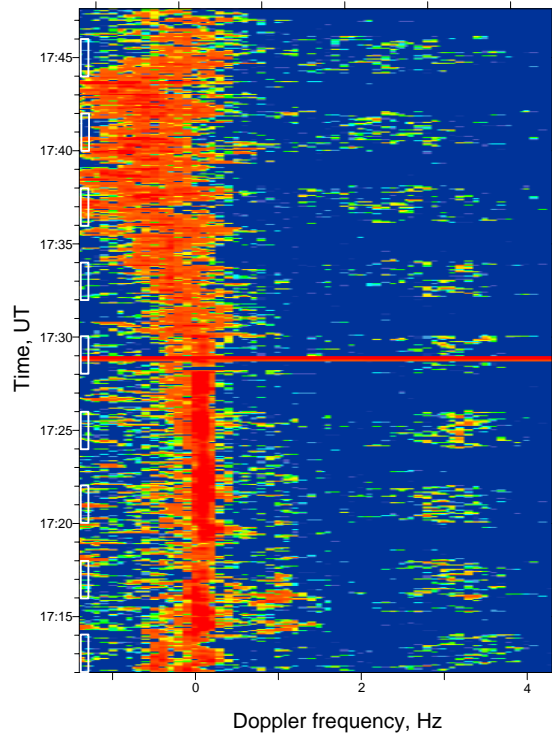


Figure 4

January 29, 2006

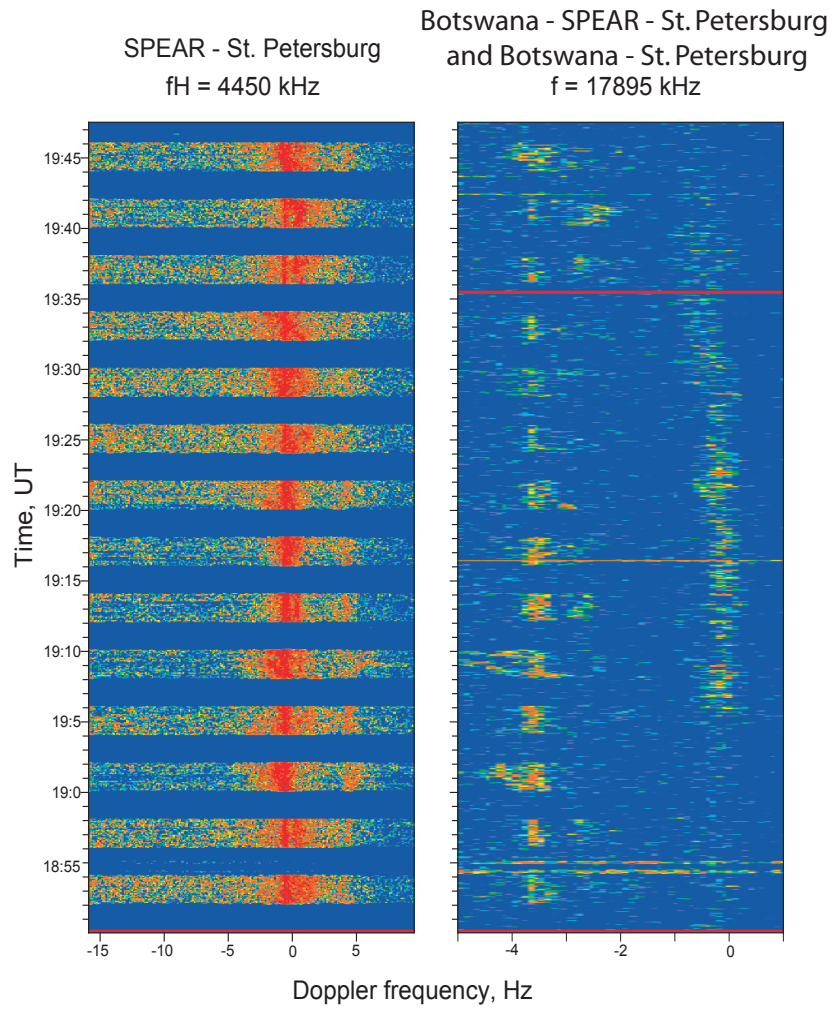


Figure 5

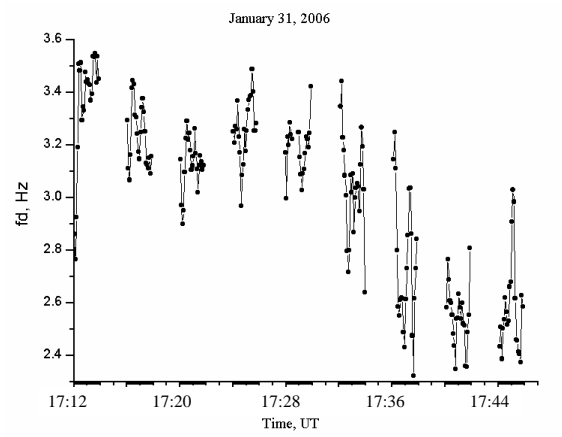


Figure 6